

# Hydrological response of a grassland invaded by Lehmann lovegrass in northern Mexico

Ramírez-Garduño, Héctor<sup>1</sup>; Sosa-Pérez, Gabriel<sup>1\*</sup>; Jurado-Guerra, Pedro<sup>1</sup>; Villarreal-Guerrero, Federico<sup>2</sup>; Hernández-Quiroz, Nathalie S.<sup>2</sup>; Ochoa-Cárdenas, Carlos<sup>3</sup>

<sup>1</sup> Campo Experimental La Campana, Instituto Nacional de Investigaciones Forestales, Agrícolas y Pecuarias (INIFAP), km 33.3 Carretera Chihuahua-Ojinaga, Aldama, Chih. 32910, México.

<sup>2</sup> Facultad de Zootecnia y Ecología, Universidad Autónoma de Chihuahua, Periférico Fco. R. Almada km 1, Chihuahua, Chih. 31453, México.

<sup>3</sup> Ecohydrology Lab, College of Agricultural Sciences, Oregon State University, Corvallis, OR, USA.

\* Correspondence: sosa.gabriel@inifap.gob.mx

## ABSTRACT

**Objective:** To calculate the runoff ratio, sediment yield, and infiltration capacity in an open bunchgrass grassland invaded by Lehmann lovegrass in northern Mexico.

**Design/methodology/approach:** The runoff-rainfall ratio, infiltration capacity, and the sediment yield were calculated using the simulated rainfall approach. Each simulation (n=20) lasted 30 min and involved two runs (*i.e.*, dry and wet).

**Results:** Differences were non-significant for the analyzed variables. The dry run showed a runoff-rainfall ratio of 0.32, and an infiltration capacity of 112 mm h<sup>-1</sup>, whereas the wet run recorded a runoff-rainfall ratio of 0.39 and an infiltration capacity of 96.9 mm h<sup>-1</sup>. Regarding sediment yield, a mean of 59.8 g m<sup>-2</sup> and 53.8 g m<sup>-2</sup> were recorded for the dry and the wet runs, respectively.

**Limitations on study/implications:** Our rainfall simulator use a single nozzle connected to a water pump where is difficult to control the two rainfall properties of a natural rainfall event (rainfall intensity and drop-size characteristics). Therefore, the high application rate does not necessarily correspond to high-intensity storm characteristics if the drop size and velocity are reduced.

**Findings/conclusions:** Soil moisture content, soil bulk density, slope, and depth were determining factors in the hydrological response of this grassland. The runoff ratio was relatively low, even for the wet runs, suggesting that the sandy loam texture of the soil favors infiltration rates and that this effect is much higher than the ground cover effect in an invaded grassland.

**Keywords:** infiltration capacity, sediment yield, simulated rainfall.

**Citation:** Ramírez-Garduño, H., Sosa-Pérez, G., Jurado-Guerra, P., Villarreal-Guerrero, F., Hernández-Quiroz, N. S., & Ochoa-Cárdenas, C. (2025). Hydrological response of a grassland invaded by Lehmann lovegrass in northern Mexico. *Agro Productividad*. <https://doi.org/10.32854/v9fvfn75>

**Academic Editor:** Jorge Cadena Iñiguez

**Associate Editor:** Dra. Lucero del Mar Ruiz Posadas

**Guest Editor:** Daniel Alejandro Cadena Zamudio

**Received:** June 29, 2025.

**Accepted:** October 17, 2025.

**Published on-line:** December XX, 2025.

*Agro Productividad*, 19(11). November. 2025. pp: 25-36.

This work is licensed under a Creative Commons Attribution-Non-Commercial 4.0 International license.



## INTRODUCTION

Grasslands play a crucial role in soil conservation and hydrological regulation. They provide various environmental services, such as carbon sequestration, control of soil erosion, and flood mitigation [1]. However, pressures such as overgrazing, conversion of land to agriculture, and drought [2][3] render these ecosystems vulnerable to degradation by water erosion [4]. As a consequence, native grasses are often replaced by exotic species,

leading to ecosystem alterations [5]. In northern Mexico, two of the most common invasive species are Natal grass (*Melinis repens* (Willd.) Zizka) and Lehmann lovegrass (*Eragrostis lehmanniana* Nees). Both are adapted to semiarid climates with low precipitation and degraded soils [6]. Prior studies have shown that invasive species can alter surface water flow paths and affect soil water retention [7], as well as influence soil structure, infiltration, and runoff processes [8]. They also exacerbate erosion and soil loss by modifying vegetation cover and reducing aggregate stability [9]. Lehmann lovegrass is a perennial bunchgrass adapted to northern Mexico, thriving on colluvial soils under semi-arid conditions with limited rainfall [10]. This species has been extensively studied in terms of morphology [11], seedling emergence and survival [12], forage production [13], expansion and distribution potential [14], and environmental impact [15]. However, hydrological investigations focused on *E. lehmanniana* addressing water balance [16], soil evaporation [17], runoff, sediment yield, and infiltrability remain limited [18][19][20][21]. Indeed, hydrologic assessments in northern Mexican rangelands invaded by this grass are scarce or absent.

Rainfall simulation is a widely used technique in diverse ecosystems for studying infiltration, runoff, and soil erosion [22]. By mimicking the characteristics of natural precipitation, it enables evaluation of how rainfall intensity and duration affect soil stability, and how vegetation cover or management practices influence soil conservation. For example, a rainfall simulation comparing buffelgrass (*Pennisetum ciliare*) with native grasslands found higher final infiltration rates in the buffelgrass site ( $50.40 \text{ mm h}^{-1}$ ) compared to the native grassland ( $38.80 \text{ mm h}^{-1}$ ), attributed to denser grass cover and litter [23]. Another study examining exotic grasses observed that Lehmann lovegrass retained less water and produced more runoff than native species [19]. Despite these insights, there is a dearth of information on the hydrological behavior of soils dominated by Lehmann lovegrass. Most research has centered on its ecological effects and competition with native flora, rather than its hydrological implications. This study aims to characterize the hydrological response of a bunchgrass-dominated system under *E. lehmanniana*, in terms of runoff coefficients, infiltration capacity, and sediment yield, using rainfall simulations under two soil moisture regimes in Chihuahua, Mexico. Our guiding question is: How do runoff coefficient, infiltration capacity, and sediment yield vary in a Lehmann lovegrass-dominated grassland under dry and wet soil conditions? This investigation offers novel insights into the hydrological behavior of Lehmann lovegrass in semi-arid grasslands.

## MATERIALS AND METHODS

The study was conducted at La Campana Experimental Ranch, part of the “Instituto Nacional de Investigaciones Forestales, Agrícolas y Pecuarias” (INIFAP), located at kilometer 80 on the Chihuahua-Juárez highway in the state of Chihuahua, Mexico (Figure 1). The elevation of the study area ranges from 1,500 to 1,800 meters above sea level. Over the past decade (2014-2024), the average annual precipitation has been 317 mm, with a mean annual temperature between 12 and 17 °C. The climate is classified as semi-arid temperate. Geologically, the region is dominated by alluvial deposits, with some areas featuring conglomerate formations. The primary soil types include skeletal Regosols and episkeletal Phaeozems, both with coarse textures and stony surfaces [24]. The general soil

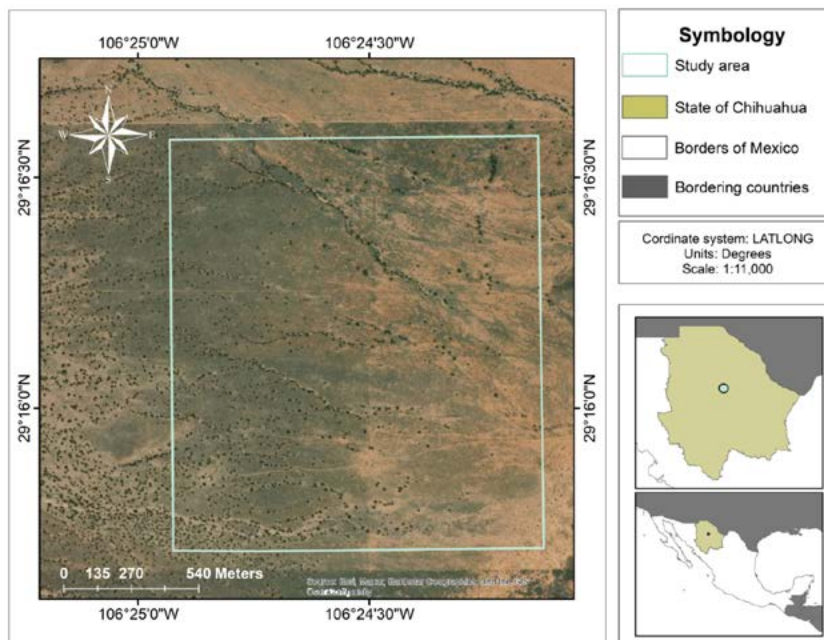


**Figure 1.** Study area at “La Campana” Experimental Ranch in Chihuahua, México.

texture is loamy-sandy to sandy-loam. Vegetation at the site is dominated by Lehmann lovegrass (*Eragrostis lehmanniana*), along with species of Muhlenbergia and Arizona oak (*Quercus arizonica* Sarg.) [25] (Figure 2). The site has been subject to continuous grazing by rodeo cattle and equines for the past 15 years, with an approximate stocking rate of 0.3 animal units (AU) per hectare.



**Figure 2.** Lehmann lovegrass grassland at “La Campana” Experimental Ranch.

Rainfall simulations were conducted from May to June 2024 using a rainfall simulator designed to replicate natural precipitation. The simulator featured a metal tripod equipped with a ¼ G10 sprinkler nozzle (Spraying Systems Co., Wheaton, IL), mounted vertically at a height of 2 meters above a 1 m<sup>2</sup> circular metal ring (Figure 3). This setup allowed for a uniform distribution of raindrops over the designated test area. Ten 1 m<sup>2</sup> plots were randomly selected for testing. Prior to each simulation, the circular metal ring was installed by driving it 5 cm into the soil using a sledgehammer and wooden block, aligning it with the slope direction to replicate natural runoff flow. The simulator was powered by a ¼ horsepower (HP) motor pump, which was connected to a 1,000-liter water tank. Each plot was subjected to two rainfall simulations: one under dry soil conditions and another under wet conditions, conducted 24 hours after the dry simulation. This resulted in a total of 20 rainfall simulation events (10 plots × 2 conditions), enabling the evaluation of hydrological behavior under both moisture scenarios.

Before and after each rainfall simulation, several physical and hydrological variables were measured to characterize the soil and vegetation conditions of each plot, including soil moisture, ground cover, slope, soil depth, soil bulk density, and soil texture. Soil moisture was recorded before each simulation using a TDR 100 probe (Spectrum Technologies) with 3.8 cm short rods, due to the rocky soil conditions. Measurements were taken at five points located 10 cm outside the edge of the ring. Ground cover was assessed using the point-intercept method, with two 1-meter transects placed 20 cm from the ring's edge, along the slope direction on both sides. The slope was measured using a 1-meter nylon string and a string level. Soil depth was measured after the wet simulation using a graduated rod at 20 cm intervals along two 1-meter transects oriented north-south and east-west. Soil bulk density was calculated using the volume excavation method, and soil texture was determined from samples collected from the top 20 cm of each plot.

Each simulation lasted 30 minutes, with rainfall and runoff data collected every 3 minutes. Rainfall was measured using two wedge-type plastic rain gauges placed inside the



**Figure 3.** Rainfall simulator used to determine runoff, infiltration, and sediment yield.

ring, 20 cm from opposite edges. Rainfall intensity ranged from 110 mm h<sup>-1</sup> to 255 mm h<sup>-1</sup>, with a mean of 184 mm h<sup>-1</sup>. The high rainfall intensity was intentionally used to assess sediment yield response. Runoff dynamics were also recorded, including runoff initiation time (elapsed time until runoff began), final runoff time (when runoff ceased), and time to peak runoff (time to reach maximum runoff rate). Runoff volume was measured with a 250 mL or 1,000 mL graduated cylinder, depending on the flow. The runoff-rainfall ratio (RR) was calculated as the proportion of rainfall resulting in runoff by dividing the total runoff by the total rainfall in the plot. Infiltration rate was estimated as the difference between rainfall and runoff, while infiltration capacity was modeled using the Horton infiltration equation:

$$f(t) = f_c + (f_0 - f_c) * e^{-kt}$$

where:  $f(t)$  is the infiltration capacity at time ( $t$ ),  $f_0$  is the initial infiltration capacity ( $t=0$ ),  $f_c$  is the constant or equilibrium infiltration capacity (steady infiltration rate),  $k$  is the decay constant (representing the decrease in infiltration capacity over time), and  $t$  is time. The Horton equation was solved using Solver in Excel to determine the optimal value, considering the aforementioned parameters.

A one-liter runoff sample, or the total runoff volume when less than one liter, was collected from each simulation plot for sediment yield analysis, resulting in 10 samples per soil moisture condition. Sediment yield was determined using the Imhoff cone method [29]. The main variables reported from each simulation included runoff initiation (minutes), final runoff time (minutes), time to peak runoff (minutes), runoff rate (mm h<sup>-1</sup>), runoff ratio, infiltration capacity (mm h<sup>-1</sup>), and sediment yield (g m<sup>-2</sup>). To assess the effect of soil moisture conditions (dry *vs.* wet), paired samples t-tests were performed using R software (R Core Team, 2024). The normality of the differences was evaluated with the Shapiro-Wilk test. For variables that did not meet the normality assumption, the Wilcoxon signed-rank test was applied as a non-parametric alternative. Relationships between hydrological response variables: runoff ratio, infiltration capacity, sediment yield, and plot characteristics (sand content, bulk density, soil moisture content, slope, soil depth, and rainfall intensity) were examined using Pearson correlation, simple linear regression, and multiple regression models. These analyses were conducted using the “mrl” and “tidyverse” packages in R. To determine the relative contribution of each plot characteristic to the hydrological responses, the “relaimpo” package was used.

## RESULTS AND DISCUSSION

Ground cover in the study area was primarily composed of bare soil (48%), followed by litter (35.5%), Lehmann lovegrass (8%), and herbaceous vegetation (5.5%). The soil was classified as sandy loam in texture, with bulk density ranging from 1.45 to 1.77 g cm<sup>-3</sup>. Slopes across the plots varied from 4% to 16%, while soil depth ranged from 10.8 to 34.88 cm.

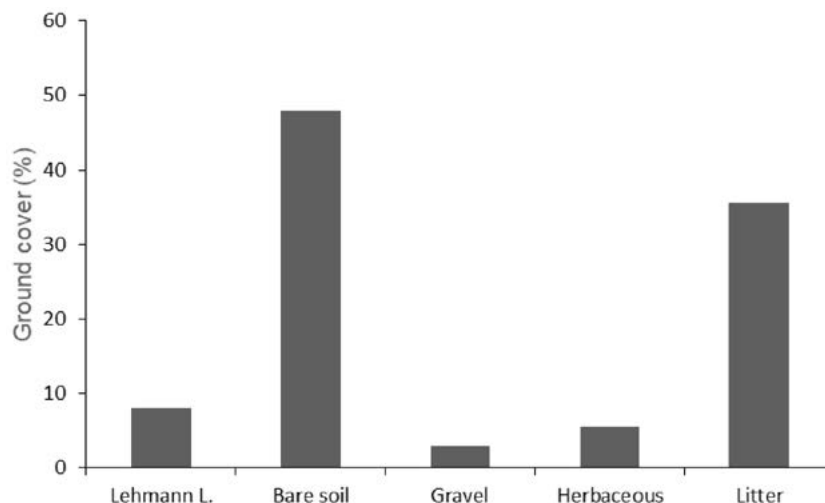


**Figure 4.** Ground cover in a Lehmann lovegrass grassland in Chihuahua, México.

### Runoff

The runoff-rainfall ratio (RR) did not differ significantly between dry and wet simulations ( $p=0.201$ ) (Table 1). Despite the high rainfall intensities ( $189 \text{ mm h}^{-1}$  in the dry run and  $181 \text{ mm h}^{-1}$  in the wet run), the RR values were only 32% and 39%, respectively. In the

**Table 1.** Summary statistics of runoff, infiltration, and sediment yield under dry and wet runs.

Dry	Mean	Standard Deviation	Minimum	Maximum
Runoff initiation (min)	1.95	1.89	0.23	6.57
Time to peak runoff (min)	24.82	4.51	15.00	30.00
Final runoff (min)	1.40	0.35	0.97	1.95
Rainfall ( $\text{mm h}^{-1}$ )	188.64	32.70	139.50	234.30
Runoff ( $\text{mm h}^{-1}$ )	60.94	23.39	24.59	91.62
Runoff ratio	0.32	0.10	0.13	0.47
Sediment yield ( $\text{g m}^{-2}$ )	51.75	38.26	13.51	102.76
Infiltration capacity ( $\text{mm h}^{-1}$ )	111.53	26.49	54.96	149.79
Final sediment ( $\text{g m}^{-2}$ )	1.49	1.38	0.11	3.68
<b>Wet</b>				
Runoff initiation (min)	1.79	1.43	0.47	5.40
Time to peak runoff (min)	20.40	5.06	15.00	30.00
Final runoff (min)	1.36	0.31	0.87	1.87
Rainfall ( $\text{mm h}^{-1}$ )	181.25	45.99	110.00	255.00
Runoff ( $\text{mm h}^{-1}$ )	73.44	38.12	32.12	145.26
Runoff ratio	0.39	0.12	0.27	0.57
Sediment yield ( $\text{g m}^{-2}$ )	53.77	56.05	13.51	170.00
Infiltration capacity ( $\text{mm h}^{-1}$ )	96.89	21.90	67.40	135.60
Final sediment ( $\text{g m}^{-2}$ )	1.04	1.54	0.11	5.00

dry run, runoff initiated on average at  $1.95 \pm 1.89$  minutes and peaked at 24.8 minutes; in the wet run, initiation occurred at  $1.79 \pm 1.43$  minutes and the peak at 20.40 minutes. Both scenarios had similar durations of final runoff (Table 1). The absence of statistical differences indicates that soil texture likely influenced the RR. Sandy loam soils (60-70 % sand) are known to favor drainage, even under intense rainfall conditions applied 24 hours later in this experiment [31][32].

In a Lehmann lovegrass invaded grassland, [19] reported an RR of 0.6, classifying it as prone to runoff. They observed maximum runoff of  $31 \text{ mm h}^{-1}$  in dry runs and  $39 \text{ mm h}^{-1}$  in wet runs under a rainfall intensity of  $45 \text{ mm h}^{-1}$ . Another simulation near our site, with comparable ground cover and a mean rainfall intensity of  $115 \text{ mm h}^{-1}$ , found an RR of 0.73 under dry conditions and 0.90 under wet conditions [33]. A separate Lehmann lovegrass study reported a maximum runoff of  $135 \text{ mm h}^{-1}$  under a precipitation intensity of  $178 \text{ mm h}^{-1}$  [21]. Additionally, investigations into soil stability in sites with mesquite and Lehmann lovegrass invasions reported a runoff coefficient of 0.60 [20]. These prior studies [19][21] used different simulator setups and larger ( $12 \text{ m}^2$ ) runoff plots compared to our design.

Contrary to earlier observations, our results suggest that ground cover had little effect on RR, as partial dependence plots showed no discernible trends and none of the predictor variables emerged as significant in multiple regression models. Therefore, the relatively low RR observed in this work appears to be more strongly controlled by soil texture than by vegetation cover.

### **Infiltration Capacity**

There were no statistically significant differences in infiltration capacity (IC) between the dry and wet runs ( $p=0.580$ ). Overall, the average IC was  $112 \pm 26.5 \text{ mm h}^{-1}$  under the dry run and  $96.9 \pm 21.9 \text{ mm h}^{-1}$  under the wet run. During the dry run, infiltration began at  $161 \text{ mm h}^{-1}$  and declined exponentially, reaching an asymptote at minute 21 ( $\text{IC} \approx 118 \text{ mm h}^{-1}$ ) (Figure 5; Table 1). In the wet run, infiltration began slightly higher at  $165 \text{ mm h}^{-1}$  but dropped sharply to  $118 \text{ mm h}^{-1}$  by minute 6, with the asymptote reached at minute 18 ( $\text{IC} \approx 97 \text{ mm h}^{-1}$ ) (Figure 5). The pronounced drop in infiltration during the wet run is consistent with observations in semiarid regions, where infiltration rates are strongly influenced by initial soil moisture levels [34]. It is well documented that soils with lower moisture content yield higher infiltration capacities [35]. Hu *et al.* (2010) analyzed how initial soil moisture affects infiltration across different rainfall intensities and found that infiltration rates tend to decrease as soil moisture increases. In our case, the abrupt decline in IC might also be attributed to the high rainfall intensity, which can rapidly saturate soil pores and reduce infiltration—even in coarse-textured soils [37]. Previous studies in grasslands invaded by Lehmann lovegrass recorded saturated hydraulic conductivity (Ks) values around  $25 \text{ mm h}^{-1}$  [19], which are markedly lower than our IC asymptotes. Another study using a mini-disk infiltrometer at a similar site reported an average IC of  $43.56 \text{ mm h}^{-1}$  [38]. Although IC and Ks reflect related but distinct hydraulic properties, the asymptotic infiltration capacity often approximates Ks, since infiltration declines with time as the soil becomes saturated [39]. The discrepancy in

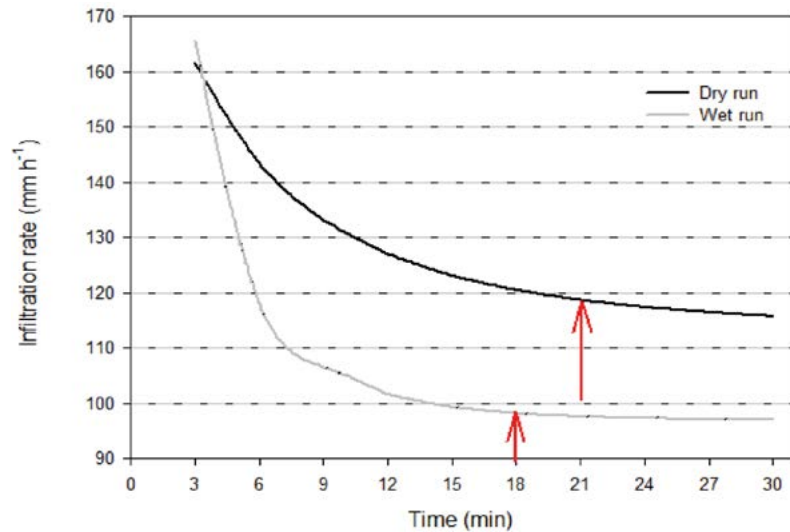


**Figure 5.** Average infiltration rate in a Lehmann lovegrass grassland. Red arrows indicate the asymptote at a determined time.

values likely reflects methodological differences (rainfall simulation vs. infiltrometer) and underscores the notably high infiltration potential at our site. One notable observation is the considerable variability in infiltration rates in both dry and wet runs. Numerous factors govern the dynamic interplay between infiltration rates and soil moisture, and high variability is common even under identical rainfall conditions [40] or within locations having the same soil and vegetation characteristics [41]. One influential parameter is bulk density, a key determinant of hydraulic conductivity [42]. Our bulk density ranged from 1.45 to 1.77 g cm<sup>-3</sup>, which may partly explain the observed variability. Although these values are somewhat higher than those typically reported for open grasslands (~1.42 g cm<sup>-3</sup>) [43], they remain within the acceptable range for plant growth [44]. Similar to runoff behavior, soil texture also plays a central role in infiltration dynamics [45]. In our study, the sandy loam texture supported high initial infiltration rates and relatively low runoff-rainfall ratios even under wet conditions and high-intensity rainfall. This finding suggests a strong potential for soil percolation and groundwater recharge in these grassland soils.

The multiple regression analysis revealed that volumetric water content and slope were the main predictors of infiltration capacity (IC) ( $R^2=0.58$ ;  $p=0.019$ ). The relative importance analysis showed that slope accounted for 56.9% of the explained variance in IC, while soil volumetric water content (SVWC) contributed 43.1%. Interestingly, IC increased with slope up to about 11%, but declined at steeper gradients. Likewise, IC was higher at low SVWC and decreased as SVWC increased. These findings align with prior work by [46], who showed that the slope infiltration relationship changes with gradient, possibly due to enhanced crust formation and increased overland flow on steeper slopes. Additionally, local factors such as soil texture, vegetation cover, and rainfall intensity also modulate infiltration behavior [47][48]. The observed decline in IC with increasing SVWC is consistent with [45], wherein higher matric potentials (*i.e.*

drier soils) favor water absorption and infiltration, whereas wetter soils with lower matric potential impede it. [49] highlighted that spatial and temporal variability in soil moisture and its interaction with hydraulic soil properties critically shapes infiltration dynamics across soil profiles.

### **Final sediment and sediment yield**

Final sediment and sediment yield (SY) did not differ between the dry and wet runs ( $p=0.735$  and  $p=0.270$ , respectively) (Table 1). The overall mean sediment yield was  $52.76 \text{ g m}^{-2}$  ( $SD=46.71$ ). We observed high variability. Multiple regression analysis identified volumetric water content, slope, and soil depth as the primary predictors of sediment yield ( $R^2=0.89$ ;  $p=0.0007$ ). The relative importance of each variable was: soil depth (41.0%), volumetric water content (31.7%), and slope (27.1%). Sediment yield decreased as soil depth increased, suggesting greater infiltration, whereas higher soil moisture content and steeper slopes favored higher sediment yield. Variables such as sand percentage and bare ground were not significant predictors at this site. In contrast, in grasslands invaded by mesquite and Lehmann lovegrass, percent soil cover and bare ground have been shown to significantly influence SY ratios [20], with lower vegetation cover and more bare soil corresponding to increased sediment production. In a prior study using  $12 \text{ m}^2$  runoff plots in mesquite/Lehmann lovegrass-invaded sites and a different rainfall simulator, the reported SY was  $16.1 \text{ g m}^{-2}$  [20]. While slope data were not given, our sediment yield coefficient was higher ( $32.95 \text{ g m}^{-2}$ ). Another investigation in a Lehmann lovegrass grassland found a sediment yield of  $23 \text{ g m}^{-2}$  at  $120 \text{ mm h}^{-1}$  over 45 minutes [21]. In contrast, a nearby study reported  $0.63 \text{ g m}^{-2}$  under a slope of 1.46% and rainfall intensity of  $52.3 \text{ mm h}^{-1}$  [33]. These comparisons underscore the strong spatial and methodological variability found in sediment yield studies.

Beyond plot characteristics, the pronounced variability in our results may also stem from rainfall intensity. The influence of rainfall on erosion processes depends on both duration and intensity [50]. Although we aimed to simulate an event comparable to a 50 year, 5 minute storm ( $\approx 220 \text{ mm h}^{-1}$ ) [51], limitations of the simulator may have produced smaller drop sizes or lower kinetic energy, resembling drizzle rather than intense storms. More sophisticated simulators (*e.g.*, Purdue-type) are often better able to reproduce natural rainfall's variable intensity and dropsize distributions [41][52]. Because our device uses a single nozzle and pump, controlling both intensity and drop kinetic energy is challenging—thus a high application rate does not necessarily equate to stormlike erosivity if drop size or velocity is reduced [53].

### **CONCLUSION**

Soil volumetric water content, slope, and soil depth were key determinants in the hydrological response, driving both infiltration capacity and sediment yield. The runoffrainfall ratio remained relatively low, even under wet conditions, indicating that the sandy loam soil texture promotes infiltration more strongly than vegetation cover influences runoff in this invaded grassland. Our results also highlight the nuanced interactions between rainfall intensity and soil characteristics, emphasizing the need for

sitespecific assessments when designing sustainable land management strategies especially in ecosystems vulnerable to vegetation change and land degradation.

## ACKNOWLEDGEMENTS

We acknowledge the financial support of INIFAP and thank Efraín Valverde for facilitating this study. We also extend gratitude to the students and faculty of the Facultad de Zootecnia y Ecología at Universidad Autónoma de Chihuahua particularly Eréndira Tiscareño (Master's student), Rosalba Chaparro (student, Universidad Tecnológica de la Tarahumara), and Irvin Gurrola for assistance with data collection and sediment analysis.

## REFERENCES

- Zhao, Y., Liu, Z., Wu, J. 2020. Grassland ecosystem services: a systematic review of research advances and future directions. *Landscape Ecology*, 35, 793-814.
- Curtin, C. G., Western, D. 2008. Grasslands, people, and conservation: over-the-horizon learning exchanges between Africa and American pastoralists. *Conservation biology*, 22(4), 870-877.
- Henwood, W. D. 1998. An overview of protected areas in the temperate grassland biome. *Parks* 8: 3-8.
- Lal, R. 2001. Soil degradation by erosion. *Land Degradation & Development*, 12(6), 519-539.
- Briske, D. D., Fuhlendorf, S. D., Smeins, F. E. 2005. State-and-transition models, thresholds, and rangeland health: a synthesis of ecological concepts and perspectives. *Rangeland Ecology & Management*, 58(1), 1-10.
- González-García, H., Sánchez-Maldonado, A., Sánchez-Muñoz, A. J., Orozco-Erives, A., Castillo-Castillo, M., Martínez-De la Rosa, R., González-Morita, J. A. 2016. Valor nutritivo del zacate rosado (*Melinis repens*) y del zacate africano (*Eragrostis lehmanniana*) en Chihuahua. *Ciencia en la Frontera*, 14(2).
- Wilcox, B. P., Turnbull, L., Young, M. H., Williams, C. J., Ravi, S., Seyfried, M. S., Wainwright, J. 2012. Invasion of shrublands by exotic grasses: ecohydrological consequences in cold versus warm deserts. *Ecohydrology*, 5(2), 160-173.
- Prevéy, J. S., Seastedt, T. R. 2014. Seasonality of precipitation interacts with exotic species to alter the composition and phenology of a semi arid grassland. *Journal of Ecology*, 102(6), 1549-1561.
- Duniway, M. C., Pfennigwerth, A. A., Fick, S. E., Nauman, T. W., Belnap, J., Barger, N. N. 2019. Wind erosion and dust from US drylands: a review of causes, consequences, and solutions in a changing world. *Ecosphere*, 10(3), e02650.
- Castillo, A. M., Nieto, M. 2013. Pasto Africano. *Gramíneas introducidas*, 53.
- Royo, M. H., Sierra, J. S., Morales, C. R., Carrillo, R. L., Melgoza, A., Jurado, P. 2008. Estudios ecológicos de pastizales. In: A. Chavez (comp). Rancho Experimental La Campana 50 años de investigación y transferencia de tecnología en pastizales y producción animal. Libro Técnico No. 2. INIFAP. Chihuahua, Mex
- Coronado, M. H. E., Castillo, A. M., Cerecedo, M. S., Romo, R. C., Castro, J. J. 2005. Emergencia y sobrevivencia de gramíneas con diferentes secuencias de humedad/sequía en tres tipos de suelo. *Técnica pecuaria en México*, 43(1), 101-115.
- Coronado, M. H. E., Romo, R. L. C. 2001. Producción de forraje y carne en pastizales resemebrados con gramíneas introducidas. *Técnica pecuaria en México*, 39(2), 139-152.
- Schussman, H., Geiger, E., Mau Crimmins, T., Ward, J. 2006. Spread and current potential distribution of an alien grass, *Eragrostis lehmanniana* Nees, in the southwestern USA: comparing historical data and ecological niche models. *Diversity and Distributions*, 12(5), 582-592.
- Sosa, M., Esqueda, M., Aguirre, C. E., Hernández, A., Lebgue, T., Soto, R. (Sin año). Evaluación del impacto ambiental del zacate africano en los pastizales centrales de Chihuahua.
- Frasier, G. W., Cox, J. R. 1994. Water balance in pure stand of Lehmann lovegrass. *Rangeland Ecology & Management/Journal of Range Management Archives*, 47(5), 373-378.
- Moran, M. S., Scott, R. L., Hamerlynck, E. P., Green, K. N., Emmerich, W. E., Collins, C. D. H. 2009. Soil evaporation response to Lehmann lovegrass (*Eragrostis lehmanniana*) invasion in a semiarid watershed. *Agricultural and Forest Meteorology*, 149(12), 2133-2142.
- Polyakov, V. O., Nearing, M. A., Nichols, M. H. 2018. Impact of long-term grazing on runoff and sediment yield in a semiarid watershed. *Journal of Soil and Water Conservation*, 73(4), 395-403.
- Viramontes-Olivas, Ó. A., Reyes-Gómez, V. M., Rangel-Rodríguez, A., Ortega-Ochoa, C., Soto-Cruz, R. A., Camarillo-Acosta, J., Lebgue-Keleng, T. 2012. Papel hidrológico-ambiental de pastizales nativos e

- introducidos en la cuenca alta del río Chuvíscar, Chihuahua, México: Hydrological and environmental role of native and introduced grasslands in the upper basin of the Chuvíscar river, Chihuahua, Mexico. *Tecnociencia Chihuahua*, 6(3), 181-193.
20. Collins, C. D. H., Stone, J. J., Cratic III, L. 2015. Runoff and sediment yield relationships with soil aggregate stability for a state-and-transition model in southeastern Arizona. *Journal of Arid Environments*, 117, 96-103.
  21. Johnson, J. C., Williams, C. J., Guertin, D. P., Archer, S. R., Heilman, P., Pierson, F. B., Wei, H. 2021. Restoration of a shrub encroached semi arid grassland: Implications for structural, hydrologic, and sediment connectivity. *Ecohydrology*, 14(4), e2281.
  22. Bowyer-Bower, T. A. S., Burt, T. P. 1989. Rainfall simulators for investigating soil response to rainfall. *Soil Technology*, 2(1), 1-16.
  23. Valle, M. A. V., Cohen, I. S., Luna, R. G., Villalobos, J. A. M., Rodríguez, H. M. 2014. Impacto hidrológico del cambio de uso del suelo de un pastizal nativo a praderas de zacate buffel (*Pennisetum ciliare* L.). *Revista Chapingo Serie Zonas Áridas*, 13(2), 47-58.
  24. Instituto Nacional de Estadística Geografía e Informática, 2024. Simulador de Flujos de Agua de Cuencas Hidrográficas. Accesado en noviembre de 2024. [https://antares.inegi.org.mx/analisis/red\\_hidro/siat/](https://antares.inegi.org.mx/analisis/red_hidro/siat/)
  25. Ramírez-Garduño, H., Hermosillo-Rojas, D. E., Sosa-Pérez, G., Jurado-Guerra, P., Hinojos-Chaparro, R. 2024. Análisis de temperatura del suelo en bosque de encino mezclado con pastizal y pastizal africano. LIX Reunión Nacional de Investigación Pecuaria. Memoria 223-225 pp.
  26. Elzinga, C. L., Salzer, D. W. 1998. Measuring & monitoring plant populations. US Department of the Interior, Bureau of Land Management.
  27. Lichter, J. M., Costello, L. R. 1994. An evaluation of volume excavation and core sampling techniques for measuring soil bulk density. *Arboriculture & Urban Forestry (AUF)*, 20(3), 160-164.
  28. Horton, R. E. 1940. An approach toward a physical interpretation of infiltration capacity. In Soil Science Society of America proceedings (Vol. 5, No. 399-417, p. 24).
  29. Sojka, R. E., Carter, D. L., Brown, M. J. 1992. Imhoff cone determination of sediment in irrigation runoff. *Soil Science Society of America Journal*, 56(3), 884-890.
  30. Ott, R. L., Longnecker, M. 2016. An introduction to statistical methods and data analysis. Cengage Learning Inc.
  31. Weil, R. R., Brady, N. C., Weil, R. R. 2017. The nature and properties of soils (Vol. 1104). London, UK: Pearson.
  32. Hillel, D. 2003. Introduction to environmental soil physics. Elsevier
  33. Ramírez Garduño, H., Sierra Tristán, J.S., Gutiérrez Ronquillo, E. 2013. La rehabilitación de agostaderos y su impacto en los escurrimientos superficiales y producción de sedimentos. Instituto Nacional de Investigaciones Forestales, Agrícolas y Pecuarias. Folleto Técnico No. 45.
  34. Fischer, C., Roscher, C., Jensen, B., Eisenhauer, N., Baade, J., Attinger, S., Hildebrandt, A. 2014. How do earthworms, soil texture, and plant composition affect infiltration along an experimental plant diversity gradient in grassland? *PLoS one*, 9(6), e98987.
  35. Alaoui, A. 2015. Modeling susceptibility of grassland soil to macropore flow. *Journal of Hydrology*, 525, 536-546.
  36. Wei, L., Yang, M., Li, Z., Shao, J., Li, L., Chen, P., Zhao, R. 2022. Experimental investigation of the relationship between infiltration rate and soil moisture under rainfall conditions. *Water*, 14(9), 1347.
  37. Alagna, V., Bagarello, V., Di Prima, S., Giordano, G., Iovino, M. 2016. Testing infiltration run effects on the estimated water transmission properties of a sandy-loam soil. *Geoderma*, 267, 24-33.
  38. Ramírez-Garduño, H., Sosa-Pérez, G., & Jurado-Guerra, P. 2023. Infiltración y humedad del suelo en bosque de encino y pastizal amacollado. XII Congreso Internacional de Manejo de Pastizales. Memoria, 255:259.
  39. Green, W. H., Ampt, G. A. 1911. Studies on Soil Physics. *The Journal of Agricultural Science*, 4(1), 1-24.
  40. Sosa-Pérez, G., MacDonald, L. H. 2017. Effects of closed roads, traffic, and road decommissioning on infiltration and sediment production: a comparative study using rainfall simulations. *Catena*, 159, 93-105.
  41. He, Z.B., Zhao, W.Z., Liu, H., Chang, X.X. 2012. The response of soil moisture to rainfall event size in subalpine grassland and meadows in a semi-arid mountain range: A case study in northwestern China's Qilian Mountains. *J. Hydrol.* 421, 183-190.
  42. Sharda, A. K. 1977. Influence of soil bulk density on horizontal water infiltration. *Soil Research*, 15(1), 83-86.
  43. Tate, K. W., Dudley, D. M., McDougald, N. K., George, M. R. 2004. Effect of canopy and grazing on soil bulk density. *Journal of Range Management*, 57(4), 411-417.

44. Shukla, M. K. 2023. Soil physics: An introduction. CRC Press.
45. Haghazari, F., Shahgholi, H., Feizi, M. 2015. Factors affecting the infiltration of agricultural soils. *International Journal of Agronomy and Agricultural Research*, 6(5), 21-35.
46. Fu, B., Wang, Y.K., Zhu, B., Wang, D.J., Wang, X.T., Wang, Y.Q., Ren, Y. 2008. Experimental study on rainfall infiltration in sloping farmland of purple soil. *Transactions of the CSAE* 24(7), 39-43 (In Chinese with English abstracts).
47. Cerdà, A., & García-Fayos, P. 1997. The influence of slope angle on sediment, water, and seed losses on badland landscapes. *Geomorphology* 18(2), 77-90.
48. Mah, M. G. C., Douglas, L. A., Ringrose-Voase, A. J. 1992. Effects of crust development and surface slope on erosion by rainfall. *Soil Science* 154, 37-43.
49. Raine, S. R., McClymont, D. J., Smith, R. J. 1998. The effect of variable infiltration on design and management guidelines for surface irrigation. ASSCI National Soils Conference.
50. de Almeida, W. S., Seitz, S., de Oliveira, L. F. C., de Carvalho, D. F. 2021. Duration and intensity of rainfall events with the same erosivity change sediment yield and runoff rates. *International Soil and Water Conservation Research*, 9(1), 69-75.
51. Isoyetas de Intensidad. Secretaría de Comunicaciones y Transportes (SCT). Accesado el 7 de febrero de 2025. <https://www.sct.gob.mx/carreteras/direccion-general-de-servicios-tecnicos/isojetas/chihuahua/>.
52. Lascano, R. J., Stout, J. E., Goebel, T. S., Gitz III, D. C. 2019. A portable and mobile rainfall simulator. *Open Journal of Soil Science*, 9(10), 207-218.
53. Lazarus, R. R., Wan Jaafar, W. Z., Alengaram, U. J., Hin, L. S. 2023. Overview of the research gaps in the rainfall simulator study. *Soil Science Society of America Journal*, 87(6), 1231-1248.

